Thin-plate spline analysis of the cranial base in subjects with Class III malocclusion

G. D. Singh*, J. A. McNamara Jr** and S. Lozanoff***

*Department of Dental Surgery and Periodontology, University of Dundee, UK, **Department of Orthodontics and Pediatric Dentistry, University of Michigan, USA and ***Departments of Anatomy and Surgery, University of Hawaii, USA

SUMMARY The role of the cranial base in the emergence of Class III malocclusion is not fully understood. This study determines deformations that contribute to a Class III cranial base morphology, employing thin-plate spline analysis on lateral cephalographs. A total of 73 children of European-American descent aged between 5 and 11 years of age with Class III malocclusion were compared with an equivalent group of subjects with a normal, untreated, Class I molar occlusion. The cephalographs were traced, checked and subdivided into seven age- and sex-matched groups. Thirteen points on the cranial base were identified and digitized. The datasets were scaled to an equivalent size, and statistical analysis indicated significant differences between average Class I and Class III cranial base morphologies for each group. Thin-plate spline analysis indicated that both affine (uniform) and non-affine transformations contribute toward the total spline for each average cranial base morphology at each age group analysed. For non-affine transformations, Partial warps 10, 8 and 7 had high magnitudes, indicating large-scale deformations affecting Bolton point, basion, pterygo-maxillare, Ricketts' point and articulare. In contrast, high eigenvalues associated with Partial warps 1–3, indicating localized shape changes, were found at tuberculum sellae, sella, and the frontonasomaxillary suture.

It is concluded that large spatial-scale deformations affect the occipital complex of the cranial base and sphenoidal region, in combination with localized distortions at the frontonasal suture. These deformations may contribute to reduced orthocephalization or deficient flattening of the cranial base antero-posteriorly that, in turn, leads to the formation of a Class III malocclusion.

Introduction

Orthodontic biomechanical therapy is often employed in the management of malocclusions, some of which may be associated with craniofacial skeletal dysplasia. A variety of malocclusions have been grouped together as Angle's Class III and, until recently (Battagel, 1993, 1994), few morphometric studies of this classification of malocclusion have been undertaken. Generally, cephalometric analyses have formed the foundations of previous studies (e.g. Ellis and McNamara, 1984) to allow the specification and localization of anatomical deformations (Moyers, 1988). The analysis of Enlow *et al.* (1969) is one example of a technique used in the clinical diagnosis of malocclusion.

Although such analyses do not determine the mechanisms of midfacial retrognathia, they can facilitate hypotheses concerning growth mechanisms that can be tested experimentally. For example, Stapf (1948) subdivided Class III deformities into typical (exhibiting mandibular overgrowth) and atypical (exhibiting a diminutive maxilla). He suggested that normal and Class III malocclusions were hafted to the cranium orthognathically or retrognathically, and that craniofacial hafting determined the severity of Class III deformities. He thus developed two theories; the first that growth beyond normal limits leads to size changes and, second, that alterations in growth patterns lead to shape changes associated with a Class III appearance concomitantly.

Developmental processes associated with Class III malocclusion were documented by Sarnat (1983). He noted cartilaginous growth at the septo-presphenoidal joint and reported other growth sites of the maxillary complex such as the fronto-maxillary, zygomatico-maxillary and pterygo-maxillary sutures, resulting in divergent downward growth of the pterygoid processes and a downward shift of the hard palate, probably related to growth of the cartilaginous nasal septum. Sarnat (1983) also suggested that retardation of antero-posterior facial growth can be induced by a lag in development of the cranial base. This hypothesis contrasts with the work of Ellis and McNamara (1984) who noted that a prognathic mandibular appearance can be due to a shortening and angular bending of the cranial base. Earlier, Sanborn (1955) reported that the anterior cranial base (S–N) was shorter in Class III malocclusion, giving rise to increased SNA and craniomandibular angles. However, these findings contrast with those of Guyer *et al.* (1986) who noted that the length S–N is larger at age 5–7 years and that the posterior cranial base (S–Ba) is longer in Class III malocclusion. In addition, these authors reported that although a decreased SNA angle was demonstrable, there were no differences in either the cranial base angle (NSBa) or saddle angle (SNAr) when Class I and Class III malocclusion were compared. Therefore, although the hypotheses of Sarnat (1983) and Ellis and McNamara (1984) are not necessarily in conflict since both studies refer to a reduced cranial base angle, the characteristics of Class III malocclusion appear to exhibit heterogeneity, and the developmental sites responsible for these differences require comprehensive delineation.

Aside from cephalometry, newer morphometric methods such as superimposition techniques, Euclidean distance matrix analysis and finite element morphometry can be applied to the study of craniofacial anomalies, including malocclusions (for review see Rohlf and Marcus, 1993). Registration-free analyses, relying upon the relative positions of homologous landmarks, are preferable to those that derive linear and angular measures from coordinates (Bookstein, 1982). For example, Trenouth (1993) compared fixed relations between anatomical points and centres of gravity (centroids) and reported that normalization reduces the amount of migration of points with time. He suggested that anatomical points show greater intrinsic variation than centroids but measurements derived from their fixed relations less so. Other methods, such as multivariate analyses, are influenced by the choice of dimensions selected, whereas parameters computed upon the principles of finite element morphometry vary according to nodal points selected (Read and Lestrel, 1986). Bookstein (1978) was one of the first to apply tensor biometrics to cephalometric datasets for the analysis of skeletal change, and later for cranial shape comparison in craniofacial deformities (Bookstein, 1984). More recently, Bookstein (1989) has developed further geometrical analyses for morphospace, to fit the differences in positions of landmarks in one form relative to their positions in another (thin-plate spline transformations). Others, notably Rohlf (1993), have applied these techniques to biomorphic problems. Thin-plate spline transformation produces a geometric description of shape differences that can be decomposed into a series of components ranging in scale from features that span the entire form to features that are highly localized (Swiderski, 1993).

The analysis of thin-plate splines produces a rigorous quantitative analysis of the spatial organization of shape change (Swiderski, 1993). Thin-plate splines express the differences in two configurations of landmarks as a continuous deformation, using regression functions in which homologous data points are matched exactly between forms, explicitly to minimize the bending energy (Richtsmeier *et al.*, 1992). Bending energy can be thought of as the energy that would be required to bend an infinitely thin metal plate over one set of landmarks so that the height over each landmark is equal to the coordinates of the corresponding point in the other form; the specific interpolation function is a mathematical expression for the deformation of theoretically idealized thin metal plates (Bookstein, 1989). These properties enable the construction of transformation grids such as those associated with Thompson (1917). In

addition, the deformation can be decomposed into a series of geometric components; affine and non-affine changes. The affine transformations correspond to changes due to size difference, rotation and uniform shape change. The non-affine changes correspond to non-uniform or local deformation; each component is a weighted combination of landmark displacements. Moreover, if the objects are two-dimensional, these non-affine changes can be inspected visually for biological interpretations (Richtsmeier *et al.*, 1992).

The non-affine changes can be decomposed further into a series of more localized components represented by Partial warps, components corresponding to deformations at different geometric scales. The number of these Partial warps is three fewer than the number of landmarks (Bookstein, 1989, 1991; Swiderski, 1993). The most global components are combinations that represent transformations affecting the entire form. The other components represent a series of transformations affecting progressively smaller regions, down to highly localized changes affecting the immediate vicinity of a few closely spaced landmarks (Swiderski, 1993). The mode of each Partial warp is determined by the configuration of landmarks in the starting form, and represents the mode of relative landmark displacements for shape changes at that scale of localization. These modal forms are called the principal warps; eigenvectors of the bending energy matrix (Bookstein, 1989). Therefore, the contribution of change at the scale of a particular principal warp to the realized landmark displacements in the x,y plane is expressed as a vector; the Partial warp, i.e. the multipliers of the eigenvectors (the thin-plate spline weighted sums of the principal warps), are the Partial warps. Eigenvalues are interpreted at an inverse index to the scale of the corresponding principal warp; more energy is required to bend the thin-plate between closely spaced landmarks. Therefore, eigenvalues are inversely related to the spatial scale of the feature; high eigenvalues are associated with highly localized features and high bending energy. As magnitude is a measure of how important a principal warp is for fitting the

second form, Partial warps with large magnitudes are interpreted as making the most difference (Zelditch *et al.*, 1992, 1993). For these Partial warps, the bending energy is the product of the magnitude of the warp and its eigenvalue (Bookstein, 1989, 1991). Thus, principal warps are geometric terms in which morphological differences can be described, and Partial warps are the values assigned to them (Swiderski, 1993).

There are no studies employing thin-plate spline transformation in the examination of the aetiology of Class III malocclusion. The overall aim of this study was to provide evidence for the theory that deficient horizontalization of cranial base angulation (orthocephalization), presumably due to premature synostosis, is associated with the development of Class III malocclusions. Therefore, the specific objective of this investigation was to undertake a thin-plate spline analysis of cranial base morphology to localize primary morphological sites and their contributions, if any, to Class III malocclusion in several age groups. This paper will test the hypothesis that a specific pattern of cranial base morphology is associated with Class III malocclusion and that visualization of those deformations is feasible using thin-plate spline analysis.

Materials and methods

Seventy-three pre-treatment lateral cephalographs of patients with a Class III molar malocclusion between the ages 5 and 11 years were retrieved (Guyer *et al.*, 1986). A further 69 cephalographs were selected from untreated subjects with a Class I molar occlusion. The sample included an equal number of male and female patients of the same ethnic group, with a negative history of airway problems, and no obvious vertical skeletal problems. The sexes at each of seven age groups were combined to maximize samples, and in order to detect age-wise differences. Therefore, each group of Class III malocclusion or normal occlusion consisted of approximately 10 children, with equal numbers of males and females in each group. Following cross-sectional sample
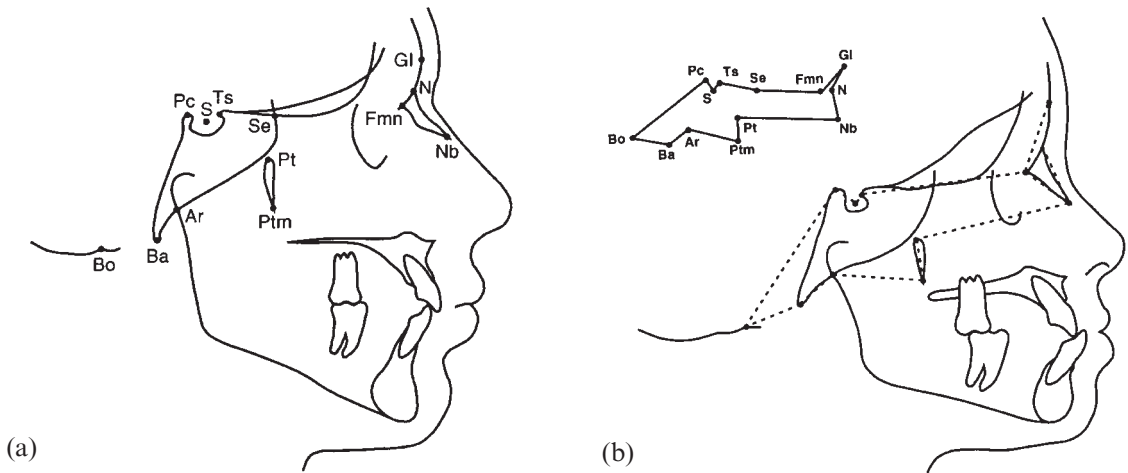
Figure 1 (a) Tracing showing the 13 cranial landmarks digitized and employed in this study superimposed on an outline produced from a Class I cephalographic profile. Definitions of landmarks employed: Ar, articulare (intersection of the condyle and the posterior cranial base); Ba, basion (lowest point on the anterior border of foramen magnum); Bo, Bolton point (highest point behind the occipital condyle); Fmn, frontonasomaxillary suture; Gl, glabella (most prominent point on the frontal bone); Pc, posterior clinoid process (most superior point); N, nasion (most anterior point on frontonasal suture); Nb, tip of nasal bone; Pt, Ricketts' point (postero-superior point on outline of pterygomaxillary fissure); Ptm, pterygo-maxillare (most inferior point on outline of pterygomaxillary fissure); S, sella (centre of sella turcica); Se, sphenoidale (intersection of the greater wings of the sphenoid and the anterior cranial base); Ts, tuberculum sellae (most anterior point of sella turcica). (b) Tracing showing the cranial configuration derived from landmarks digitized and employed in this study superimposed on an outline produced from a Class III cephalographic profile. The inset shows the outline of the cranial configuration.

construction, the relatively small samples were tested for normality and equivalence of variance. Statistical tests indicated that 94 per cent of the cranial variables reflected normality based upon Wilk's statistic ($w > 0.9$), and Levene's test showed that 99 per cent of the cranial variables showed equivalence of variance between age-wise samples. Hence, our groupings conformed to assumptions of normality and equivalence of variance, warranting further cross-sectional, geometric analysis.

The magnification of each film was standardized to an 8 per cent enlargement factor. The chronological age was assumed to match developmental age in this study as carpal ages were unavailable. Each lateral cephalograph was traced on frosted acetate film (0.03 inches thick) and checked by one investigator (G.D.S.). Digitization of landmark coordinates from cephalographs taped to a light box of uniform brightness was achieved using appropriate software and a digitizing tablet (Numonics Inc., Montgomeryville, PA). Thirteen homologous

cranial base landmarks were digitized, encompassing cranial developmental sites (Figure 1a), and located in the mid-sagittal plane where possible (Varjanne and Koski, 1982; Bhatia and Leighton, 1994). Any landmarks that demonstrated a discrepancy of more than 1 per cent for each x,y coordinate on duplicate digitization were deemed to be identified unreliably and were excluded from the final analyses. For the analysis of geometric transformation from a normal to a Class III cranial base configuration, scaled, mean cranial base morphologies for normal and Class III forms at each age were employed (Figure 1b). Prior to thin-plate spline examination, cranial base configurations were analysed for statistical significance using Procrustes analysis (Gower, 1975) and multivariate analysis (Hotelling's T^2: Bookstein, 1991; Goodall, 1991). Cranial configurations of the mean forms were subjected to thin-plate spline analysis using appropriate software (Rohlf, 1994). Each total spline was decomposed into an affine and non-affine component. The affine
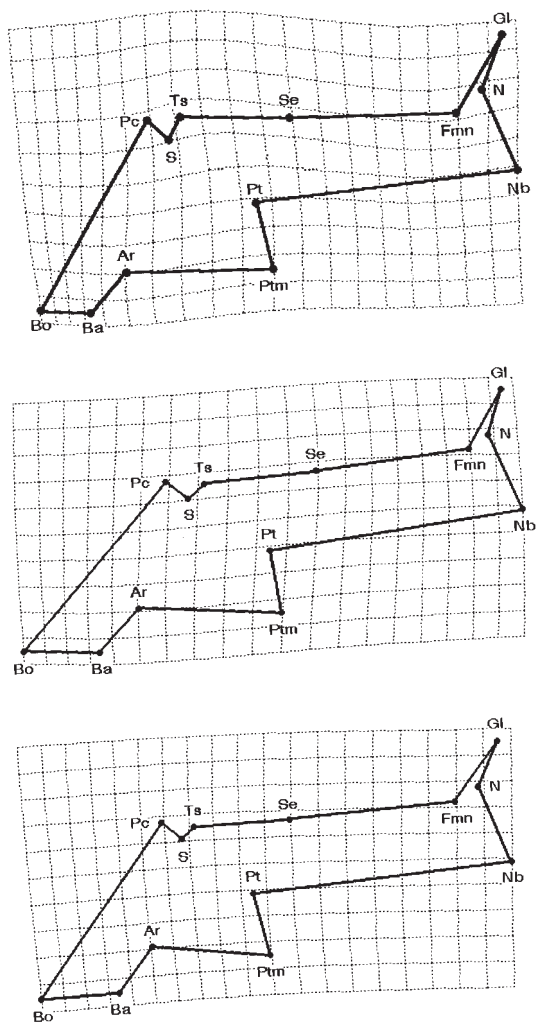
Figure 2 Graphical display showing total spline (affine and non-affine transformation components) derived from averaged normal and Class III malocclusion cranial base morphologies at age 5 years. Note the compression in the posterior region of the cranial base, expansion of the sphenoidal complex, and downward deformation of the anterior cranial base. Partial warps 10 and 8 are also illustrated.

transformation describes the uniform component of change and, requiring no 'geometrical work', has no bending energy. However, the non-affine component can be decomposed further into Partial warps, the magnitude representing the importance of the Partial warp to the total fit. Deformations of the cranial base were interpreted on this basis.

Results

Thin-plate spline analysis enabled visualization of the changes that occur in the transformation from an average, normal cranial base to an average, Class III morphology. Initial multivariate analysis indicated that, for this particular sample, statistical differences existed between the normal and Class III cranial base morphologies at all age groups tested (Table 1). On further analysis, both affine and non-affine transformations were found to contribute towards the total splines (Figures 2–8 and Tables 2–8). Decomposition into Partial warps provided descriptions of morphological deformities of the cranial base from normal to Class III configuration, and allowed localization of those deformations.

For the 5-year-old group, the total spline indicated compression in the horizontal axis in the region of the posterior cranial base, affecting Bolton point and basion. However, vertical expansion, particularly of the sphenoidal complex, and downward deformation of the anterior cranial base were also evident (Figure 2). Partial warp 10 had the highest magnitude; its large spatial scale was confirmed by its small bending energy value. Partial warp 8 also had a moderately large magnitude. In contrast, Partial warps 1 and 2 had high eigenvalues, indicating small spatial-scale (localized) deformations predominantly. These small, highly localized changes were characterized by a high bending energy (Table 2).
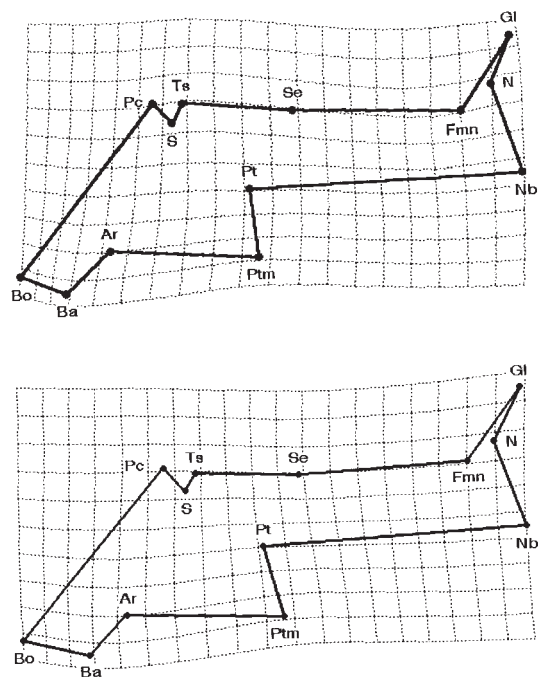
For the 6-year-old group, the total spline indicated vertical and horizontal compression of the posterior region of the cranial base (Figure 3). Although some expansion was evident in the mid-cranial region, the anterior-most region of the cranial base demonstrated a most marked upward and forward deformation. Partial warps 7 and 10 had the highest magnitudes. In contrast, Partial warps 1 and 2 had high eigenvalues; the small spatial scale of these warps was characterized by large bending energies (Table 3).

For the 7-year-old group, the total spline indicated horizontal compression (most noticeable on the superior aspect) of the posterior region of the cranial base, with vertical stretching at basion (Figure 4). While the mid-cranial region showed
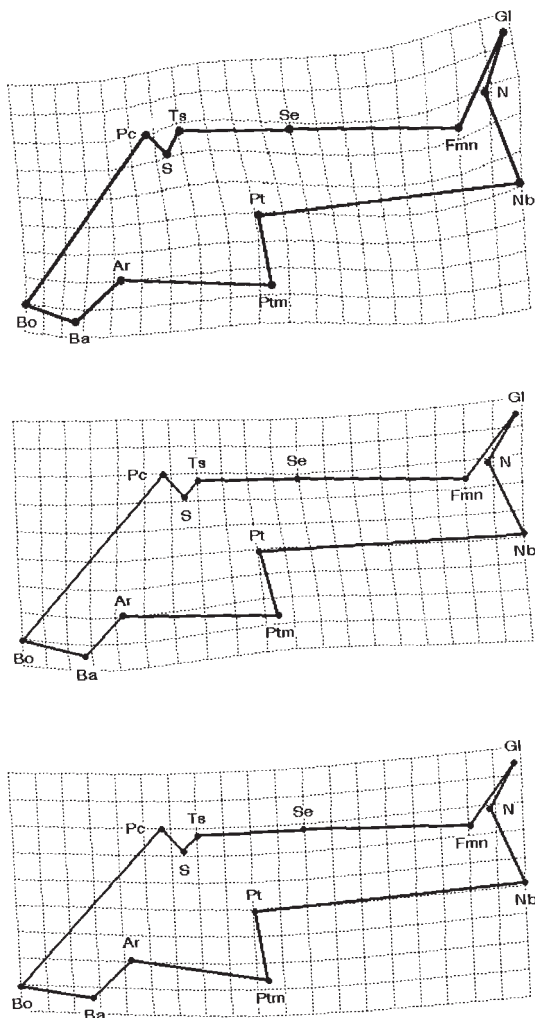
Figure 3 Graphical display showing total spline (affine and non-affine transformation components) derived from averaged normal and Class III malocclusion cranial base morphologies at age 6 years. Note the compression of the posterior region of the cranial base. Expansion is evident in the mid-cranial region but the anterior region of the cranial base demonstrates a marked upward and forward deformation. Partial warps 7 and 10 are also illustrated.

Figure 4 Graphical display showing total spline (affine and non-affine transformation components) derived from averaged normal and Class III malocclusion cranial base morphologies at age 7 years. Note the compression of the posterior region of the cranial. The mid-cranial region shows upward expansion but the anterior cranial base demonstrates a downward deformation. Partial warp 7 is also illustrated.

some upward expansion, the anterior cranial base demonstrated a downward deformation. Partial warp 7 had the highest magnitude. Partial warp 10 had the lowest bending energy (Table 4), contrasting with Partial warps 1 and 2 that had high bending energies and high eigenvalues.

For the 8-year-old group, the total spline indicated a forward compression and downward displacement of the posterior region of the cranial base, most evident between Bolton point and basion (Figure 5). While the mid-cranial region showed a mild forward expansion, an inferior deformation of the anterior cranial base was also present. Partial warps 10 and 8 had the highest magnitudes. In contrast, Partial warps 1 and 2 had high eigenvalues, but Partial warp 3 the lowest bending energy (Table 5).

For the 9-year-old group, the total spline indicated a marked forward compression of the posterior region of the cranial base, particularly at Bolton point and basion (Figure 6). While the mid-cranial region showed a mild forward expansion, an inferior deformation of the anterior cranial base at the frontonasomaxillary suture was also evident. Partial warp 10 had the

Table 1 The *F* values derived from Procrustes analysis indicate statistical differences at all ages groups, except age 7 which marginally failed. Hotelling's T^2 indicates statistical differences for either linear or angular parameters, if not both, at most age groups.
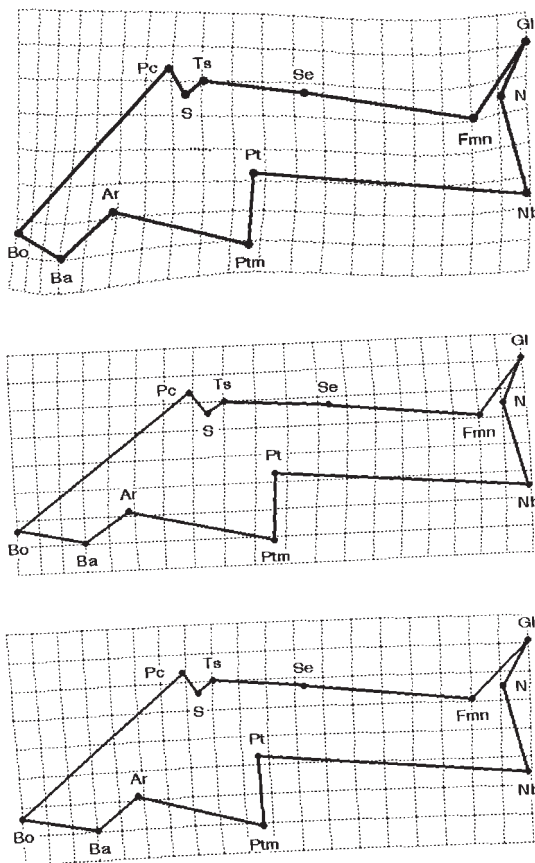
Age	Procrustes		Hotelling's T^2			
	F value	*P* value	Linear	*P* value	Angular	*P* value
5	4.512	0.001	88.15	0.0001	42.46	0.0031
6	1.756	0.010	21.06	0.0939	31.06	0.0373
7	1.432	0.100	32.36	0.0148	5.64	0.5558
8	3.353	0.001	96.89	0.0001	206.04	0.0001
9	3.795	0.001	46.34	0.0001	28.67	0.0049
10	1.482	0.050	21.75	0.0374	8.91	0.3000
11	1.870	0.005	10.71	0.1211	30.09	0.0123

Table 2 Contribution of each Partial warp towards the total spline of mean normal and Class III cranial base geometries at age 5 years. The Partial warps with large magnitudes (contributing to large spatial-scale changes in form) are marked with an asterisk.

Partial warp	Eigenvalue	Bending energy ($\times 10^3$)	Magnitude ($\times 10^5$)
1	274.764	8.562	3.116
2	178.377	4.824	2.704
3	83.827	2.017	2.407
4	48.943	1.045	2.135
5	36.541	2.460	6.732
6	22.658	1.807	7.976
7	14.453	6.594	45.628
8*	**7.650**	**5.381**	**70.346**
9	6.279	0.160	2.546
10*	**1.329**	**1.601**	**120.547**
Total	674.820	34.452	

Figure 5 Graphical display showing total spline (affine and non-affine transformation components) derived from averaged normal and Class III malocclusion cranial base morphologies at age 8 years. Note the compression and downward displacement of the posterior region of the cranial base. The mid-cranial region shows expansion but inferior deformation of the anterior cranial base. Partial warps 10 and 8 are also illustrated.

highest magnitude. In contrast, Partial warps 1, 2 and 3 had high eigenvalues (Table 6).

For the 10-year-old group, the total spline indicated a forward compression of the posterior region of the cranial base (Figure 7) somewhat similar to the total spline for the 5-year-old group (Figure 2). However, the mid-cranial region showed a large upward expansion, and an inferior deformation of the anterior cranial base predominantly at the frontonasomaxillary suture

was also evident. Partial warp 8 had the highest magnitude. In contrast, Partial warps 1, 2 and 3 had high eigenvalues (Table 7).

For the 11-year-old group, the total spline indicated some compression of the posterior region of the cranial base in the horizontal plane (Figure 8). However, although the mid-cranial region showed some upward expansion, an inferior deformation of the anterior cranial base, predominantly localized at the frontonaso-maxillary suture, was the dominant feature for this age group. Partial warps 8 and 6 had the

Table 3　Contribution of each Partial warp towards the total spline of mean normal and Class III cranial base geometries at age 6 years. The Partial warps with large magnitudes (contributing to large spatial-scale changes in form) are marked with an asterisk.

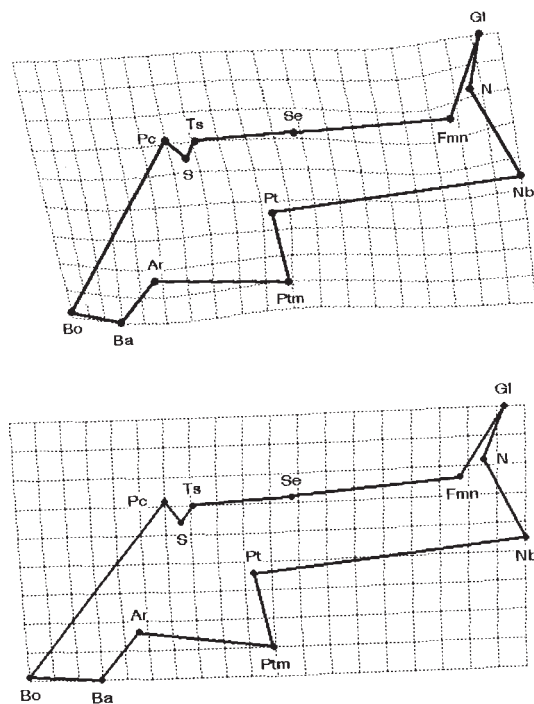| Partial warp	Eigenvalue	Bending energy $(\times 10^3)$	Magnitude $(\times 10^5)$
1	219.524	8.777	3.998
2	214.767	10.671	4.968
3	84.149	5.690	6.761
4	50.838	4.333	8.523
5	34.855	2.814	8.073
6	22.930	1.660	7.238
7*	**15.623**	**8.343**	**53.399**
8	8.985	0.980	11.013
9	6.562	0.750	11.430
10*	**1.493**	**0.774**	**51.865**
Total	659.636	44.790	

Table 4　Contribution of each Partial warp towards the total spline of mean normal and Class III cranial base geometries at age 7 years. The Partial warps with large magnitudes (contributing to large spatial-scale changes in form) are marked with an asterisk.

Partial warp	Eigenvalue	Bending energy $(\times 10^3)$	Magnitude $(\times 10^5)$
1	247.647	1.360	0.549
2	165.789	5.959	3.594
3	88.022	3.159	3.588
4	54.794	4.209	7.682
5	33.220	1.668	5.020
6	22.383	0.336	1.500
7*	**15.120**	**8.993**	**59.479**
8	8.530	1.943	22.784
9	6.139	0.463	7.541
10	1.446	0.220	15.178
Total	643.091	28.309	

Figure 6　Graphical display showing total spline (affine and non-affine transformation components) derived from averaged normal and Class III malocclusion cranial base morphologies at age 9 years. Note the compression of the posterior region of the cranial base. The mid-region shows expansion but an inferior deformation of the anterior cranial base is also evident. Partial warp 10 is also illustrated.

highest magnitudes. In contrast, Partial warps 1, 2 and 3 had high eigenvalues (Table 8), indicating small spatial-scale (localized) deformations of the cranial base.

Discussion

Battagel (1994) considers that Class III mal-

occlusions pose special clinical problems because of the tendency of relapse. In this study, a thin-plate spline analysis (Bookstein, 1991; Rohlf, 1994) was undertaken to visualize deformations and to provide insights into the localization of any anatomical kyphosis of the cranial base in subjects with Class III malocclusions. The thin-plate spline function fits the differences in the positions of landmarks in one form relative to their positions in another (Rohlf and Marcus, 1993). This method models shape difference as a deformation between landmarks; technical details are provided in Bookstein (1989, 1991). Thin-plate spline analysis is not coordinate-free but, similar to other morphometric techniques such as tensor analysis (Battagel, 1993, 1995), depends upon landmark selection. The interpolation used in spline analysis can be described by a physical metaphor in which the landmarks
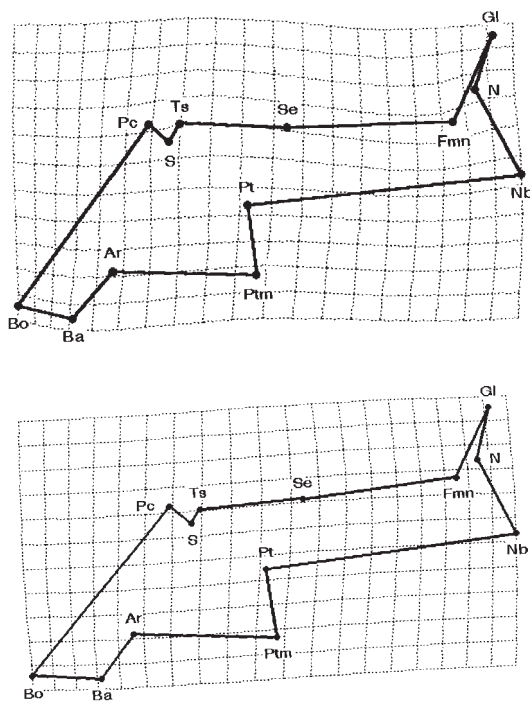
Table 6 Contribution of each Partial warp towards the total spline of mean normal and Class III cranial base geometries at age 9 years. The Partial warps with large magnitudes (contributing to large spatial-scale changes in form) are marked with an asterisk.

Partial warp	Eigenvalue	Bending energy ($\times 10^3$)	Magnitude ($\times 10^5$)
1	222.046	1.622	0.731
2	172.761	13.576	7.858
3	112.796	1.289	1.143
4	46.335	0.090	0.194
5	33.914	4.381	12.917
6	21.412	0.156	0.727
7	14.734	3.494	23.716
8	8.196	2.918	35.602
9	6.273	0.091	1.442
10*	**1.338**	**0.981**	**73.302**
Total	639.806	28.600	

Table 7 Contribution of each Partial warp towards the total spline of mean normal and Class III cranial base geometries at age 10 years. The Partial warps with large magnitudes (contributing to large spatial-scale changes in form) are marked with an asterisk.

Partial warp	Eigenvalue	Bending energy ($\times 10^3$)	Magnitude ($\times 10^5$)
1	313.934	3.565	1.136
2	128.980	12.897	10.000
3	99.558	4.609	4.629
4	48.804	2.370	4.856
5	35.285	1.073	3.042
6	20.141	0.005	0.026
7	14.346	2.406	16.771
8*	**8.148**	**5.352**	**65.682**
9	5.891	0.332	5.627
10	1.346	0.369	27.426
Total	676.433	32.978	

Figure 7 Graphical display showing total spline (affine and non-affine transformation components) derived from averaged normal and Class III malocclusion cranial base morphologies at age 10 years. Note the compression of posterior region of the cranial base (similar to the total spline for the 5-year-old group). The mid-cranial region shows upward expansion, and an inferior deformation of the anterior cranial base. Partial warp 8 is also illustrated.

of one form located on an infinitely thin metal plate are deformed so that the height over each landmark is equal to the coordinates of the corresponding point in the other form (Bookstein, 1989, 1991). Although this method is unable to determine whether there is a statistical difference between mean configurations, it allows the visualization of the differences as a grid whether these are statistically significant or not. To determine whether normal and Class III cranial bases are morphologically different, therefore, we relied upon residuals of homologous landmarks (Procrustes analysis; Gower, 1975) and multivariate analysis (Hotelling's T^2: Bookstein, 1991; Goodall, 1991). These analyses indicated that the average cranial base morphologies for normal and Class III malocclusion employed in this study are statistically significantly different. Thin-plate spline analysis is also suitable for three-dimensional studies, but was only employed in this investigation on two-dimensional data derived from lateral cephalographs.

Growth of the cranial base is variable and complex; differential growth and significant

Table 8 Contribution of each Partial warp towards the total spline of mean normal and Class III cranial base geometries at age 11 years. The Partial warps with large magnitudes (contributing to large spatial-scale changes in form) are marked with an asterisk.

Partial warp	Eigenvalue	Bending energy ($\times 10^3$)	Magnitude ($\times 10^5$)
1	264.704	3.834	1.448
2	165.422	6.318	3.891
3	100.078	1.009	1.008
4	53.352	2.164	4.055
5	33.721	3.834	11.368
6*	**23.695**	**15.529**	**65.536**
7	15.290	1.637	10.707
8*	**9.032**	**6.287**	**69.606**
9	5.643	0.035	0.619
10	1.419	0.287	20.228
Total	672.356	40.932	

differential timing of decelerations complicate allometry (Moyers, 1988). Indeed, parameters of growth may behave differently from parameters of deformation. Enlow *et al.* (1969) noted that linear measurements from cephalographs are often less important than the actual amount of growth contributing to an anatomical distance. Therefore, the analysis undertaken in this study relied upon accurate digitization of homologous landmarks and their relative positions in registration-free morphospace. However, although it was assumed that the cephalographs selected were representative of normal and Class III malocclusion, no comparisons to ideal datasets were undertaken nor was any emphasis placed upon the heterogeneic nature of the Class III grouping (Battagel, 1994). Nevertheless, our groupings conformed to assumptions of normality and equivalence of variance, warranting the assumption that for this relatively small sample, the landmarks selected were representative of cranial base morphology even though some of these were para-sagittal in location (Bhatia and Leighton, 1994). Despite these drawbacks, our results compare favourably with some earlier studies confined to cephalometrics.
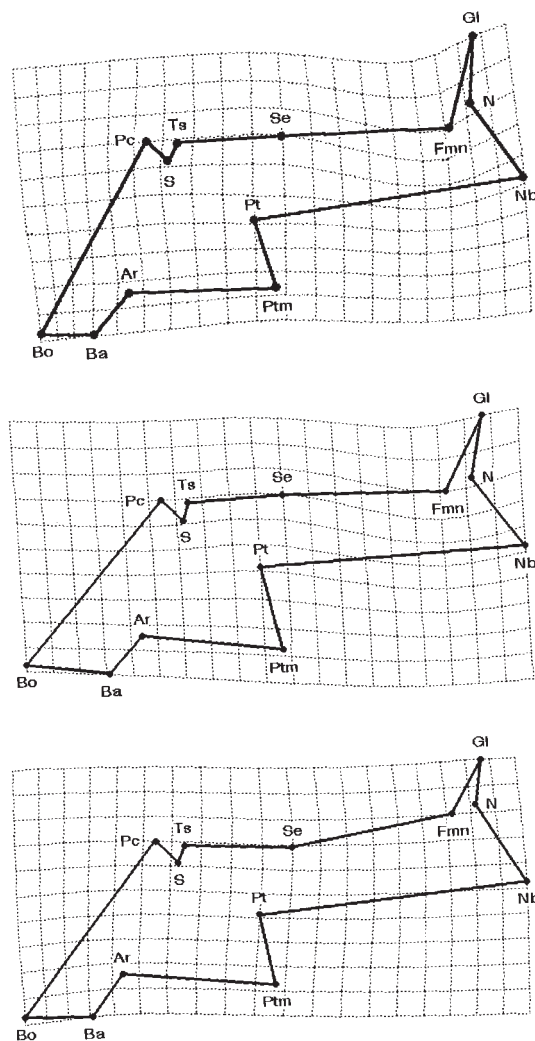
Figure 8 Graphical display showing total spline (affine and non-affine transformation components) derived from averaged normal and Class III malocclusion cranial base morphologies at age 11 years. Note the compression of the posterior region of the cranial base in the horizontal plane. The mid-cranial region shows expansion but an inferior deformation of the anterior cranial is the dominant feature. Partial warps 8 and 6 are also illustrated.

Anterior cranial base

During normal cranial base growth, Hoyte (1991) reports that elongation of the anterior cranial fossa ceases by about 10 years of age. For subjects with Class III malocclusions, Sanborn (1955) found that the anterior cranial base was shorter than normal, giving rise to increased

SNA and craniomandibular angles. In contrast, Guyer *et al.* (1986) reported that S–N is larger for Class III cases at age 5–7 years than for Class I subjects that comprise the so-called 'Bolton Standards' (Broadbent *et al.*, 1975). By identifying small, spatial-scale Partial warps, we were able to describe deformations localized predominantly at nasion and the frontonaso-maxillary suture in all age groups studied. These Partial warps indicate that shearing, upward stretching, displacement and bending of the anterior cranial base can occur. In addition, for the 11-year-old group, Partial warps 8 and 6 had the highest magnitudes, affecting the frontonasomaxillary suture and glabella, indicating a downward and forward deformation of the anterior cranial base. Sarnat (1983) noted cartilaginous growth at the septo-presphenoidal joint and reported other growth sites of the maxillary complex such as the fronto-maxillary suture. Decomposition of spline transformations graphically demonstrates regions of change within the anterior cranial base, and we are able to suggest that these deformations, at least in part, distinguish the attainment of a Class III morphology.

Mid-cranial base

Melsen (1974) found that growth activity persists in the spheno-ethmoidal suture up to 8 years of age, but growth in the spheno-occipital synchondrosis normally continues until 12–18 years (Melsen, 1972). According to Hoyte (1989), changes in the sphenoidal complex are slow from 5 to 8 years, and virtually cease by 10 years of age (Hoyte, 1991). For all age groups studied, Partial warps with high magnitudes affected pterygo-maxillare, Ricketts' point and the spheno-ethmoidal point. These points correspond with the pterygoid plates, and the floor and body of the sphenoid, respectively. These Partial warps indicated an expansion in the mid-region of the cranial base due to upward and downward stretching, and bending. Although we would argue that such changes contribute to significantly different Class I and Class III cranial base morphologies, Battagel (1993), employing tensor analysis, was unable to demonstrate such differences. However, Sarnat (1983) identified the pterygo-maxillary suture as

a growth site, resulting in divergent downward growth of pterygoid processes. Our results also indicate that significant changes occur in the mid-region of the cranial base for the development of Class III malocclusions. Furthermore, for all age groups studied, Partial warps 1–3 had high eigenvalues, predominantly localized at tuberculum sellae and sella, indicating shearing, upward stretching, upward bending, posterior displacement, and compression. Therefore, in addition to shortening of the cranial base, a prognathic mandibular profile also can be due to changes in the sphenoidal complex. These assertions are in accord with the findings reported by Sarnat (1983); significant deformations in the region of the body of the sphenoid are evident.

Posterior cranial base

Early studies suggest that the length of the cranial base is involved in the aetiology of Class III malocclusions (Hopkin *et al.*, 1968). It is likely, therefore, that some of the differences noted in this study are also allied with the changes in morphology of the posterior cranial base. For all age groups studied, the Partial warps with the highest magnitudes affected Bolton point, basion and articulare. These deformations indicated compression in the horizontal axis in the occipital region of the posterior cranial base in all age groups studied, as well as bending, vertical stretching and narrowing. Dietrich (1970) suggested two possible aetiological factors for Class III malocclusion. First, positional cause; due to a skeletal shape change that would be reflected in cephalometric angles. Second, quantitative cause; due to a size change that would be reflected in linear measurements. Our results are in accord with such hypotheses. However, Sarnat (1983) also suggested that retardation of antero-posterior facial growth can be induced by a lag in development of the cranial base. Therefore, this study contrasts with the notion suggested by Sarnat (1983) since it appears that Class III malocclusion would seem to depend upon a combination of divergent cranial base morphology anteriorly, and localized regions of dysplasia further posteriorly. Indeed, Hoyte (1991) notes that developmental mechanisms within the petro-occipital complex account for

elongation of the posterior cranial fossa, and mechanisms of antero-posterior growth could affect cranial base angulation (Hoyte, 1975). Therefore, a developmental deficiency, depicted by the deformations that we observed for the posterior region of the cranial base, could be associated with the development of a prognathic mandibular profile.

Conclusions

Large spatial-scale deformations affect the posterior region of the cranial base and the body of the sphenoid (Partial warps 8 and 10; Tables 2–8) in nearly all age groups tested, whereas localized shearing is more apparent at sella turcica than the frontonasal suture (Partial warps 1 and 2; Tables 2–8). In this study the hypothesis that a specific pattern of cranial base morphology is associated with Class III malocclusion was tested, and those deformations have been visualized using thin-plate spline analysis. Thus, a combination of large-scale and localized deformations appear to contribute to a cranial base geometry that may reflect the biological mechanisms responsible for the differences in craniofacial morphology for Class I and Class III subjects. Zelditch *et al.* (1993) suggests that, in young mammals, the cranial base straightens by an increase in the ventral angle between the basioccipital and basisphenoid bones. In our study, based upon human cephalographs, both moderate deformations in the sphenoidal region of the mid-cranial base and significant changes affecting the occipital region of the cranial base, predominantly associated with the retention of a relatively acute cranial base angle, could be identified. That the deformation of the posterior cranial base is a significant component of Class III malocclusion is supported by the magnitudes of the Partial warps describing those transformations. In this study, the theory that alteration in growth patterns leads to shape changes associated with a Class III appearance has been partly vindicated and, moreover, we are able to suggest that the alteration is likely to be a deficient orthocephalization, i.e. a failure of sufficient antero-posterior horizontalization in cranial

base angulation. However, it could not be determined whether growth below normal limits within the cranial base, presumably due to premature synostosis, leads to the changes in form identified.

Additional algorithms are available to facilitate the analysis of variation in shape for landmark data, and regression of Partial warps against factors such sex and age, etc. (Rohlf, 1993). In view of the mixed nature of the sample employed in the present study, a further analysis to determine sexual dimorphism of the cranial base in Class III malocclusions is warranted; specifically differences occurring during puberty might be of interest. Other programs for biometric image warping are also available (Bookstein and Green, 1993, 1994), and work will be directed to applying these methods in the analysis of the aetiology of Class III malocclusion, including an analysis of the nasomaxillary and mandibular morphologies. In addition, a future study based upon finite element morphometry will enable both localization and quantification of allometry within the cranial base, and will delineate a basis for the cellular and molecular analyses required for the study of midfacial retrusion.

Address for correspondence

Dr G. D. Singh
Department of Dental Surgery and Periodontology
Dundee Dental Hospital and School
University of Dundee
Park Place
Dundee DD1 4HR
UK

References

Battagel J M 1993 The aetiology of Class III malocclusion examined by tensor analysis. British Journal of Orthodontics 20: 283–296

Battagel J M 1994 Predictors of relapse in orthodontically-treated Class III malocclusion. British Journal of Orthodontics 21: 1–13

Battagel J M 1995 Tensor analysis of facial growth in males. European Journal of Orthodontics 17: 215–229

Bhatia S N, Leighton B C 1994 A manual of facial growth: A computer analysis of longitudinal cephalometric growth data. Oxford University Press. Oxford

Bookstein F L 1978 The measurement of biological shape and shape change. Lecture Notes on Biomathematics 24. Springer-Verlag. New York

Bookstein F L 1982 On the cephalometrics of skeletal change. American Journal of Orthodontics 82: 177–198

Bookstein F L 1984 Tensor biometrics for changes in cranial shape. Annals of Human Biology 11: 413–437

Bookstein F L 1989 Principal warps: Thin-plate splines and the decomposition of deformations. IEEE Transactions of Pattern Analysis and Machine Intelligence 11: 567–585

Bookstein F L 1991 Morphometric tools for landmark data: geometry and biology. Cambridge University Press. Cambridge

Bookstein F L, Green W 1993 A feature space for Edgels in images with landmarks. Journal of Mathematical Imaging Vision 3: 231–261

Bookstein F L, Green W D K 1994 Edgewarp: a flexible program package for biometric image warping in two dimensions. Visualization 1–13

Broadbent B H Sr, Broadbent B H Jr, Golden W H 1975 Bolton standards of dentofacial developmental growth. C V Mosby Co. St. Louis

Dietrich U C 1970 Morphological variability of skeletal Class III relationships as revealed by cephalometric analysis. Transactions of the European Orthodontic Society, pp. 77–88

Ellis E, McNamara J A Jr 1984 Components of adult Class III malocclusion. Journal of Oral and Maxillofacial Surgery 42: 295–305

Enlow D H, Moyers R E, Hunter W S, McNamara J A Jr 1969 A procedure for the analysis of intrinsic facial form and growth. An equivalent-balance concept. American Journal of Orthodontics 56: 6–23

Goodall C 1991 Procrustes methods in the statistical analysis of shape. Journal of the Royal Statistical Society B53: 285–339

Gower J C 1975 Generalized Procrustes analysis. Psychometrika 40: 33–51

Guyer E C, Ellis E, McNamara J A Jr, Behrents R G 1986 Components of Class III malocclusion in juveniles and adolescents. Angle Orthodontist 56: 7–30

Hopkin G B, Houston W J B, James G A 1968 The cranial base as an etiological factor in malocclusion. Angle Orthodontist 38: 250–255

Hoyte D A N 1975 A critical analysis of the growth in length of the cranial base. In: Bergsma D (ed.) Morphogenesis and malformations of the face and brain. Birth Defects, Original Articles Series 11, Alan R Liss, New York, pp. 255–282

Hoyte D A N 1989 The role of the cranial base in normal and abnormal skull development. In: Persing J A, Edgerton M T, Jane J A (eds) Scientific foundations and surgical treatment of craniosynostosis. Williams Wilkins, Baltimore, pp. 58–68

Hoyte D A N 1991 The cranial base in normal and abnormal skull growth. Neurosurgery Clinics of North America 2: 515–537

Melsen B 1972 Time and mode of closure of the spheno-occipital synchondrosis determined on human autopsy material. Acta Anatomica 83: 112–119

Melsen B 1974 The cranial base. Acta Odontologica Scandinavica Suppl 62: 9–126

Moyers R E 1988 Handbook of orthodontics. Mosby Year Book Inc. St. Louis

Read D W, Lestrel P 1986 Comment on the uses of homologous-point measures in systematics: A reply to Bookstein et al. Systematic Zoology 35: 241–253

Richtsmeier J T, Cheverud J M, Lele S 1992 Advances in anthropological morphometrics. Annual Review of Anthropology 21: 283–305

Rohlf F J 1993 Relative warp analysis and an example of its application to mosquito wings. In: Marcus L F, Bello E, Garcia-Valedcasas A (eds) Contributions to morphometrics. Museo de Ciencias Naturales, pp. 131–159

Rohlf F J 1994 TPSpline, life.bio.sunysb.edu, or Professor FJ Rohlf, Department of Ecology and Evolution, StateUniversity of New York, Stony Brook, New York, USA

Rohlf F J, Marcus L F 1993 A revolution in morphometrics. Trends in Ecology and Evolution 8: 129–132

Sanborn R T 1955 Differences between the facial skeletal patterns of Class III malocclusion and normal occlusion. Angle Orthodontist 25: 208–222

Sarnat B G 1983 Normal and abnormal craniofacial growth. Angle Orthodontist 53: 263–289

Stapf W C 1948 A cephalometric roentgenographic appraisal of the facial pattern in Class III malocclusion. Angle Orthodontist 18: 20–23

Swiderski D L 1993 Morphological evolution of the scapula in tree squirrels, chipmunks, and ground squirrels (Sciuridae): An analysis using thin-plate splines. Evolution 47: 1854–1873

Thompson D W 1917 On growth and form. The University Press. Cambridge

Trenouth M J 1993 Variation of anatomical and centroid points in the human fetal skull. Angle Orthodontist 63: 39–46

Varjanne I, Koski K 1982 Cranial base, sagittal jaw relationship and occlusion. A radiological-craniometric appraisal. Proceedings of the Finnish Dental Society 78: 179–183

Zelditch M L, Bookstein F L, Lundrigan B L 1992 Ontogeny of integrated skull growth in the cotton rat Sigmodon fuliventer. Evolution 46: 1164–1180

Zelditch M L, Bookstein F L, Lundrigan B L 1993 The ontogenetic complexity of developmental constraints. Journal of Evolutionary Biology 6: 121–141